

Numerical Simulation and Optimization of Heat Transfer in Reciprocating Flows in Two-Dimensional Channels

H. Shokouhmand, A. Mosahebi¹, and B. Karami

Abstract—Forced convection heat transfer in laminar reciprocating flow in a two-dimensional channel based on Womersley number (α), Prandtl number (Pr), Pressure gradient amplitude and cross section thickness of the channel. As characteristic length is numerically simulated using spectral element method (SEM). In flow with high α , temperature distribution is highly affected by Richardson annular effect. Although increasing α enhances heat transfer rate, but it actually reduces oscillations amplitude and flow penetration length, hence it reduces heat transfer rate. These two contradictory effects predict existence of optimum frequency for heat transfer rate in a specific geometry. In our study pressure gradient amplitude has been chosen as a design parameter rather than penetration length. At this study optimum values of frequency and geometrical parameters are investigated.

Index Terms—Numerical simulation, Reciprocating flows, Heat transfer, Optimization.

I. INTRODUCTION

Several investigations have been done on fluid flow and heat transfer in ducts and channels at both regimes of laminar and turbulent flows because of their extensive engineering and industrial applications. In spite of these cases, oscillatory flows are new and have more stringent time and spatial resolution requirements.

Some studies have been done on the oscillatory flows to enhance heat transfer rate. A general review has been recently given by Cooper et al. [1]. Since then, additional experimental results dealing with zero-mean oscillatory flows have been reported by Zhao and Cheng [2], Richardson and Tyler [3], Siegel [4] and Liao et al. [5], which all show significantly enhanced heat transfer in ducts and enclosures. Sert and Beskok, which this study is based on their work, have studied reciprocating flows in two-dimensional channels [6].

Manuscript received March 25, 2007.

H. Shokouhmand is with the School of Mechanical Engineering, University of Tehran, P.O. Box 11365/4562, Tehran, Iran (corresponding author to provide phone: +98(21)-88005677; fax: +98(21)-88013029; E-mail: hshokoh@ut.ac.ir).

A. Mosahebi is with the School of Mechanical Engineering, University of Tehran, P.O. Box 11365/4562, Tehran, Iran. (E-mail: amosahebi@ut.ac.ir).

B. Karami is with the School of Mechanical Engineering, University of Tehran, P.O. Box 11365/4562, Tehran, Iran. (E-mail: bkarami@ut.ac.ir).

Oscillatory flows can be grouped into two categories: pulsating (modulated) and reciprocating (fully reversing) flows. Pulsating flows are always unidirectional and can be decomposed into steady and unsteady components, such as in the case of blood flow in arteries. For reciprocating flows, the flow direction changes cyclically. Hence, these flows convect zero net mass.

One broad application of heat transfer is thermal management of microelectronic components, which is a challenging problem. Increase in the central processing unit (CPU) speeds is required for faster computers. However, the amounts of heat generation also increase with the increased CPU speeds. Inefficient thermal design leads to large chip surface temperatures, which severely affect the chip performance and commonly result in chip malfunction. To overcome this problem, several novel heat exchanger devices for electronic cooling applications utilize reciprocating flow and heat transfer. Reciprocating flows require interchange between the inflow and outflow boundaries during a cycle. For most applications, it is difficult to determine the inflow/outflow boundary conditions, since fluid particles exiting the flow domain during a part of the cycle are fed back into the domain, later in the cycle.

At this study momentum equation in reciprocating flow forced convection in two-dimensional channels is solved analytically. Since in general there is no analytical solution for energy equation, it has to be solved numerically. One of the high-order accurate numerical methods for solution of engineering PDE's is Spectral Element Method (SEM) [7-10]. SEM combines geometrical flexibility of finite element method and exponential convergence of spectral method. More details about SEM, is described in the next sections. At the present study, energy equation is solved using SEM. Although at this study because of simplicity of geometry, flexibility of SEM is not necessary, but exponential convergence of SEM made this method appropriate for solution of our energy equation.

II. PROBLEM DEFINITION AND MAIN PARAMETERS

In Fig.1 the geometry with imposed boundary condition is shown. In this problem we assume a fully developed flow that established by oscillatory pressure gradient. Middle zone of upper plate is warmed by constant heat flux while both side regions are in constant temperature T_0 . Bottom wall is

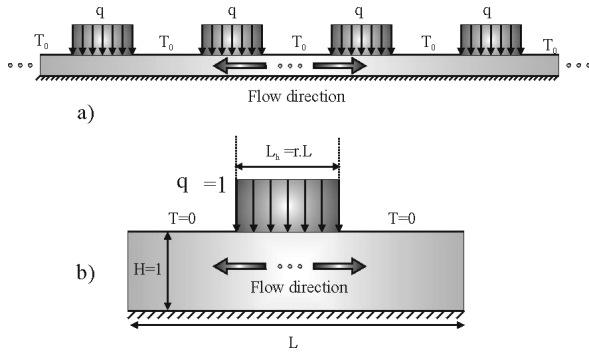


Fig. 1. The geometry and thermal boundary conditions used in this study.

insulated and for side boundaries, velocity and temperature are assumed to be periodic.

Symmetric top wall boundary conditions caused to establish periodic conditions at vertical boundaries. If shown region repeated periodically, we can assume that exited flow at righthand side of one zone is entered to the left hand side of next zone, which has equal behavior to the present zone, Fig.1-a. Hence synthetical and thermophysical parameters of fluid at both side are uniform and implementation of periodic boundary conditions is logical. For this problem five non-dimensional geometrical and thermophysical parameters are defined that describe behavior of system completely [6]. Those parameters are as follow:

$$Pr, \alpha, L_p = L^* \rho^* H^*, L_h = L^* \mu^* H^*, L = L^* / H^*$$

Two parameters L and L_h are geometrical parameters, L_p is penetration length of fluid which specifies mean displacement of fluid particles in one-half of an oscillation period $\tau^*/2$. Pr and α are parameters that describe fluid property. H^* is channel height and used as a characteristic length. Considering sinusoidal oscillations, the penetration length is defined as:

$$L_p^* = \hat{u}^* \frac{\pi}{\omega^*} = \hat{u}^* \frac{\tau^*}{2} \quad (1)$$

where L_p^* is practical measurement of oscillation amplitude and \hat{u}^* is the mean velocity in half of one period. In order to enhance heat transfer, L_p^* has to be large enough to permit warmed fluid under constant heat flux region moved toward constant temperature boundaries. In reciprocating flows, a key non-dimensional parameter is Womersley number (α), that is defined as follow:

$$\alpha = \sqrt{\frac{\omega^* H^{*2}}{\nu}} \quad (2)$$

which ν is kinematic viscosity. Womersley number specifies velocity profile shape. Small α values result a quasi-steady flow with oscillatory parabolic velocity profiles that are in same phase with pressure gradient. In large values of α , well known phenomena, i.e. Richardson annular effect is visible. This effect causes increasing velocity near walls and so maximum velocity will not be on the center of channel either. In this case particles at different situations oscillate with different phase related to pressure gradient [3]. The Womersley number is sometimes called the kinetic Reynolds

number because it plays the same role as the Reynolds number in unidirectional steady flows. Prandtl number that shows ratio of momentum and thermal diffusivities is also important in heat transfer. For reciprocating flows, the thermal boundary layer thickness is determined by both the Prandtl and Womersley numbers.

III. GOVERNING EQUATIONS

Using below non-dimensional parameters:

$$x = x^* / H^*, \quad y = y^* / H^*, \quad t = t^* \omega^*, \quad u = u^* / H^* \omega^*, \quad p = p^* / (\rho^* H^* \omega^{*2})$$

$$T = (T^* - T_0^*) / \Delta T^*, \quad q'' = q'' / (k^* \Delta T^* / H^*)$$

governing equations of problem (continuity, momentum, and energy) in the case of a two-dimensional channel with incompressible fluid and constant thermo-physical properties are obtained. The velocity has non-dimensionalized using $\omega^* H^*$ that is because of lack of a specific velocity for non-dimensionalization. T_0^* is constant temperature of wall and ΔT^* is maximum allowable temperature difference in the filed, that is one of the design parameter. Using these non-dimensional parameters, we have governing equations in non-dimensional form as follow

$$\nabla \cdot \vec{u} = 0 \quad (3)$$

$$\frac{\partial \vec{u}}{\partial t} + (\vec{u} \cdot \nabla) \vec{u} = -\nabla p + \frac{1}{Re} \nabla^2 \vec{u} \quad (4)$$

$$\frac{\partial T}{\partial t} + (\vec{u} \cdot \nabla) T = \frac{1}{Pe} \nabla^2 T \quad (5)$$

Where \vec{u} is velocity vector, $Re = \alpha^2$, $Pe = Re.Pr$ and T and P are temperature and pressure distribution, respectively. In addition fluid properties are considered to be constant. In continue, we study fully developed flow, that in result for flows in two dimensional channels, velocity has only one component in x direction and it is a function of y and t . With this assumption continuity equation is satisfied. Due attention to the assumed function for pressure gradient, the analytical solution for velocity profile can be obtained

IV. ANALYTICAL SOLUTION of MOMENTUM EQUATION

For fully developed flow, momentum equation is simplified to bellow form:

$$\frac{\partial u}{\partial t} = -\frac{dp}{dx} + \frac{1}{Re} \frac{\partial^2 u}{\partial y^2} \quad (6)$$

as illustrated, fluid is flowed oscillatory by means of pressure gradient via below relation:

$$\frac{dp^*}{dx^*} = -A^* \cos(\omega^* t^*) \quad (7)$$

Using complex function, In non-dimensional form, (7) is demonstrated as follow:

$$-\frac{dp}{dx} = \Re(A \exp(-it)) \quad (8)$$

At the above equation, A is pressure gradient amplitude that has been non-dimensionalized with $\rho^* \omega^{*2} H^*$. If velocity profile considered to be as $\Re(\omega(y) \exp(-it))$, and substituted to (6), then:

$$\frac{\omega''}{\alpha^2} + i\omega + A = 0 \quad (9)$$

By Implementation of boundary conditions for (12), velocity profile obtained as:

$$u(y, t) = \Re\{iA \exp(-it) [1 - \frac{\cos((1+i)\sqrt{2\alpha}y/2)}{\cos((1+i)\sqrt{2\alpha}/4)}]\} \quad (10)$$

Equation (10) shows non-dimensional velocity profile in terms of non-dimensional parameters y, α, t , and A . At Fig. 2, velocity profile in terms of $\alpha = 1$ and $\alpha = 10$ are presented ($L_p = 10$). Due attention to obtained velocity function, L_p is determined from the below relation

$$L_p = 2A \Re\left(1 - \frac{2\sqrt{2}}{\alpha(i+1)} \tan((1+i)\frac{\sqrt{2}}{4}\alpha)\right) \quad (11)$$

At most references for example reference [6] this parameters have been studied and results compared. In one specific geometry, the only remaining parameters are α and L_p equations 1, 2), that in previous studies were quantified independently. From the above equations observed that $\alpha \approx \sqrt{f^*}$ and $A \approx 1/F^{*2}$. Hence at high frequencies for appropriate L_p (high L_p), high pressure gradient is needed that in practical point of view is difficult.

V. NUMERICAL SOLUTION of ENERGY EQUATION

At present section energy equation has been solved numerically. We start by describing the common spatial discretization used by the SEM formulations, then continuous Galerkin formulations is presented.

A. Spatial Discretization

In SEM, the physical domain is divided into quadrilateral elements which can be mapped individually to a computational plane (ζ, η) . The solution within each element is interpolated with a high-order polynomial according to:

$$T(t, \zeta, \eta) = \sum_{i=0}^N \sum_{j=0}^N \hat{T}_{i,j}(t) \Psi_{ij}(\zeta, \eta) \quad (12)$$

where $\Psi_{ij}(\zeta, \eta)$ are the interpolation (or trial) functions in modal form, and the $\hat{T}_{i,j}$ are unknown coefficients that depend on time only and has no physical meaning. In two dimensions the interpolant consists of tensorized modified Jacobi polynomials of the form [7]:

$$\Psi_{ij}(\zeta, \eta) = h_i(\zeta) h_j(\eta) \quad (13)$$

Where, $h_i(\zeta)$ is defined as follow

$$h_i(\zeta) = \begin{cases} \frac{1-\zeta}{2} & i=0 \\ \frac{1-\zeta}{2} \frac{1+\zeta}{2} P_{i-1}^{\alpha, \beta}(\zeta) & 0 < i < N \\ \frac{1+\zeta}{2} & i=N \end{cases} \quad (14)$$

$P_{i-1}^{\alpha, \beta}(\zeta, \eta)$ is Jacobi polynomial of order i .

B. Continuous Galerkin Formulation

The weak form of the advection equation amounts to finding a T such that

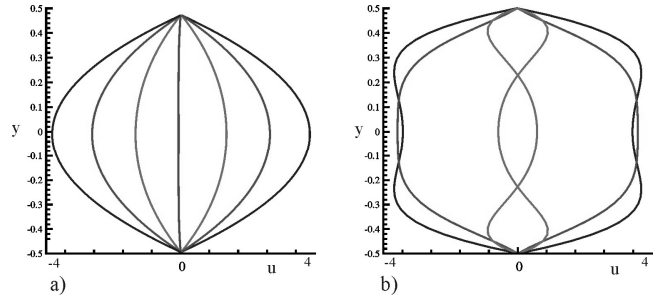


Fig. 2. Analytical solution of the velocity profiles at various times during a cycle for (a) $\alpha=1$, and (b) $\alpha=10$

$$\int_{\Omega} \Psi T(t) dA - \int_{\Omega} \Omega T \bar{u} \cdot \nabla \Psi dA = \int_{\partial \Omega_0} \Omega T \bar{u} \cdot \bar{n} dS - \int_{\partial \Omega_0} \Omega T \bar{u} \cdot \bar{n} dS \quad \forall \Psi \in H^1 \quad (15)$$

where, Ψ_i 's are weight functions belonging to the Hilbert space H^1 , and the divergence theorem has been invoked to integrate by parts the divergence term. The application of the classical Galerkin procedure leads to a discrete system of ordinary differential equations of the form $M \dot{T} - DT = f$ where T refers to the vector of unknown coefficients, M is the mass matrix, D represents the discrete divergence operator, and f is the load vector on the system.

C. Temporal Discretization

As mentioned above, implementation of Galerkin formulation to PDE's lead to system of ordinary differential equations in matrix forms. There are various methods to integrate above system of equations in both form of implicit and explicit. Third order Adams-Bashforth method because of their wide stability region and high accuracy are of interest and is implemented [10].

VI. Results validation

At this section, our results have been verified by comparing them with results of reference [6]. Two cases of [6] have been chosen with below specifications.

Case 1:

$$H^* = 1 \text{ mm}, \quad L = 22, \quad L_H = 12, \quad \alpha = 10, \quad \text{Pr} = 10$$

Case 8:

$$H^* = 1 \text{ mm}, \quad L = 22, \quad L_H = 12, \quad \alpha = 1, \quad \text{Pr} = 1$$

In Fig.3 Instantaneous temperature contours for these two cases have been compared. As it is observed, there is a good agreement between results.

VII. Results and discussion

At this section, oscillations frequency and geometry of a channel with bellow specifications are optimized.

$$H^* = 0.001 \text{ m}, \quad L = 10, \quad L_H = r \times L, \quad A^* = 1000 \text{ Pa/m}$$

Air at temperature of 25°C is considered as working fluid and its specifications assumed to be constant so:

$$\alpha = \sqrt{\frac{\omega^* H^*}{\nu^*}} = 0.6288 \sqrt{f^*} \quad (16)$$

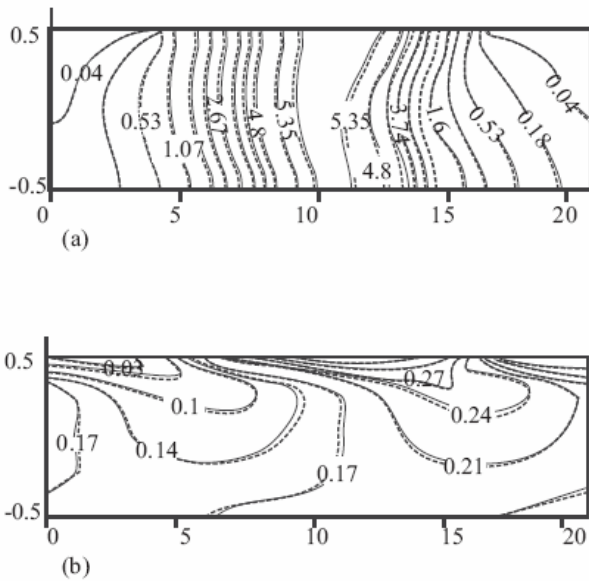


Fig. 3: Instantaneous temperature contours for cases 1 and 8 of Ref [6]. At both cases (a) and (b) dashed lines are results of Ref [6] and solid lines are numerical results of presented study.

Where f^* is oscillations frequency and α is Womersely number. Considering definition of A:

$$A = \frac{A^*}{\rho^* \omega^{*2} H^*} = \frac{21810.14}{f^{*2}} \quad (17)$$

as defined above:

$$L_p = 2A\Re \left[1 - \frac{2\sqrt{2}}{\alpha(1+i)} \tan\left((1+i)\frac{\sqrt{2}}{4}\alpha\right) \right] \quad (18)$$

Using f^* and r ($0 \leq r \leq 1$), that is the ratio of constant heat flux region to channel length; the problem can be define completely. Now appropriate values for f^* and r in order to maximize heat transfer is discussed.

At first for a constant r , frequency changed at the range of $0.001 \leq f^* \leq 1000$ and at each frequency heat flux q'' is calculated. q'' is non-dimensionalized using heat flux at a stationary fluid at the same geometry. In the case of stationary fluid only diffusion terms remain and so energy equation is reduced to Laplace equation. Defining none-dimensional variable, q''/q''_{cond} , effect of advection term in heat transfer for various frequency can be studied. These effects have been studied for various r and results have shown at Fig.4. In addition as observed from Fig. 4, by increasing r to approximately $r=0.8$, advection term, play an important role in heat transfer. For example at $r=0.8$ and optimum frequency of $f^* \approx 20$, advection term can enhance heat transfer rate nearly 9.2 times. For small and large values of r ($r \approx 0$ or $r \approx 1$), advection term is negligible because at this cases, diffusion is dominated heat transfer mechanism.

In addition from Fig. 5 observed that at very high frequencies temperature distributions are approached to stationary flow condition and effect of advection term in energy equation can be neglected. Also at very low

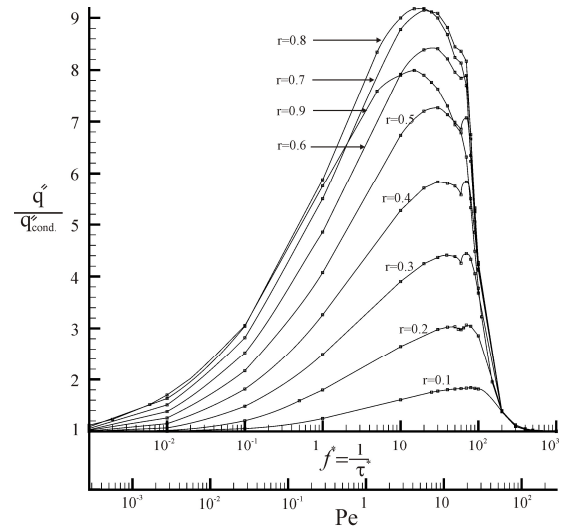


Fig 4: Effect of frequency on heat flux in various magnitudes of r .

frequencies, when flow direction is changed, velocity magnitude is nearly zero and temperature distribution will be similar to stationary flow, so we have sudden increasing of temperature. Sudden enhancement of temperature caused that for all values of r at very high and very low frequencies, values of q''/q''_{cond} have been approached to 1. At Fig.5, maximum temperature as a function of non-dimensionalized time for $r = 0.5$ and various frequency of $f^* = 0.001$, $f^* = 1.0$ and $f^* = 1000$ is represented.

As it shown in Fig. 5-a, at low frequencies, when flow direction is changed, there is sudden increasing in maximum temperature while for the other times, maximum temperature is in an appropriate range. By increasing frequency, amplitude of temperatures variations reduced and also mean value approached to greater ones. At Fig. 5-b this fact is shown. At this case, because of flow low average temperature and low temperature oscillations amplitude, maximum temperature at one period is very smaller than maximum values of Fig.5-a. At figure Fig. 5-c, oscillations frequency is very high, and as

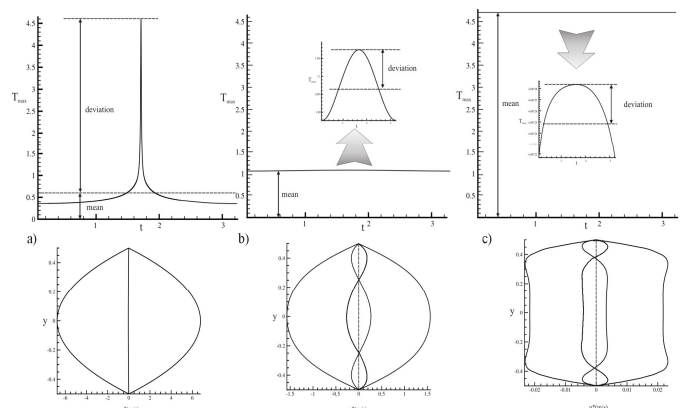


Fig 5: temperature in channel as a function of non-dimensionalized time in half of one period for $r = 0.5$ and various frequency of a) $f^* = 0.001$, b) $f^* = 1.0$ and c) $f^* = 1000$

described before, this caused to increasing mean value to maximum temperature value of stationary flow. Hence although temperature oscillations amplitude is too low, because of high mean value, appropriate condition is not observed.

At Fig.4, for each value of r , maximum allowable heat flux has been non-dimensionalized with maximum allowable heat flux of stationary flow at corresponding r . So comparison of heat transfer magnitude between different values of r is provided.

In addition maximum transferred heat is proportional to product of maximum heat flux and length of warm zone. In order to compare heat transfer of different r , we did non-dimensionalization in other way. So for each frequency transferred heat from warm surface at $r=0.5$ is used as reference value for non-dimensionalization. At Fig. 6 results of this non-dimensionalization is shown.

As it shown at very high and very low frequencies for small values of r , discharged heat is more than case of $r=0.5$. At $0.6 \leq r \leq 0.7$ for moderate frequencies heat transfer is maximum and by increasing or decreasing r , its value is reduced. It should be noticed that, although for high and low frequencies and low r , relative transferred heat is enhanced, since heat transfer rate is very low, in general, there is no important improvement in heat transfer. At moderate frequencies (as seen from Fig. 4 amount of heat transfer is very high. In order to final adding up and obtaining total optimum geometry and frequency, for optimum frequencies of different r , maximum transferred y has been non-dimensionalized with transferred heat at optimum frequency of $r=0.5$. Results are presented at Fig. 7. From this figure observed that for $r \approx 0.6$ at corresponding optimum frequency, $f^* \approx 30$, heat transfer is maximum.

Follow effects of two parameters A^* and Pr are studied. At Fig. 8 graph of q''/q''_{cond} at $r=0.5$ for different values of $A^*=100, 1000, 10000$ is presented. As shown by increasing pressure gradient amplitude (A^*), maximum heat flux enhanced and occurred at higher frequencies while by

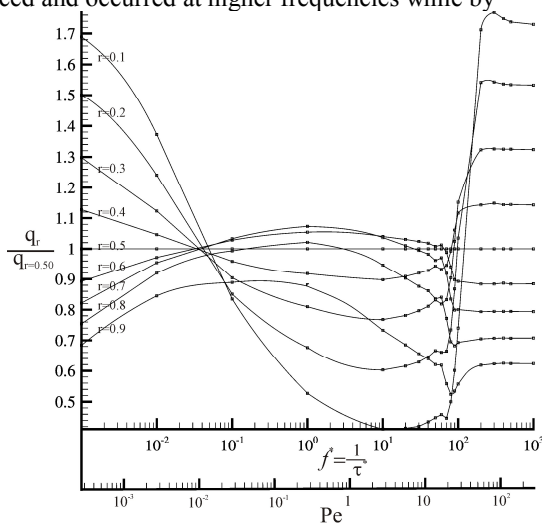


Fig 6: Effect of frequency on heat transfer in various magnitudes of r .

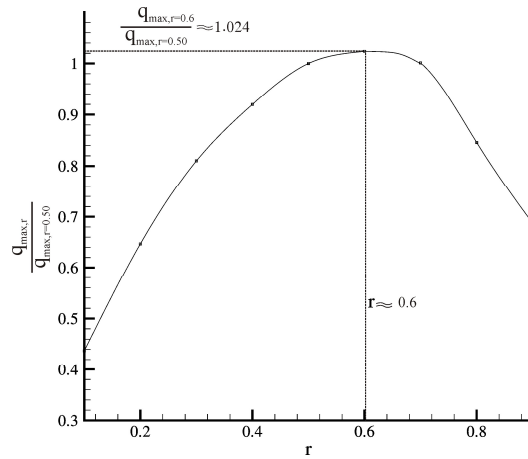


Fig 7: non-dimensionalization total heat transfer and optimum geometry.

reducing A^* this value is reduced and approached to lower frequencies. This fact is clear because by increasing pressure gradient, oscillations amplitude causes to increasing up and heat transfer is improved. In addition optimum frequency is enhanced and Richardson annular effect causes to heat transfer increasing. This matter for small values of A^* is completely reverse.

At Fig.9 effect of Pr number on heat transfer rate for $r=0.5$ is shown. At this case $Pr=0.707$. As seen increasing Pr , causes to increasing ratio of heat transfer in presence of advection term to heat transfer of stationary flow. This matter can not be seen for low Pr , i. e. reality at this case diffusion is dominant heat transfer mechanism and advection term can be neglected.

A fluid with low Pr (liquid metals) because of high heat conductivity coefficient (k^*), conduction heat transfer has more contribution in total heat transfer in comparison with fluid with high prandtel number. Also for large Pr it seems that optimum frequencies don't change and is independent of Pr .

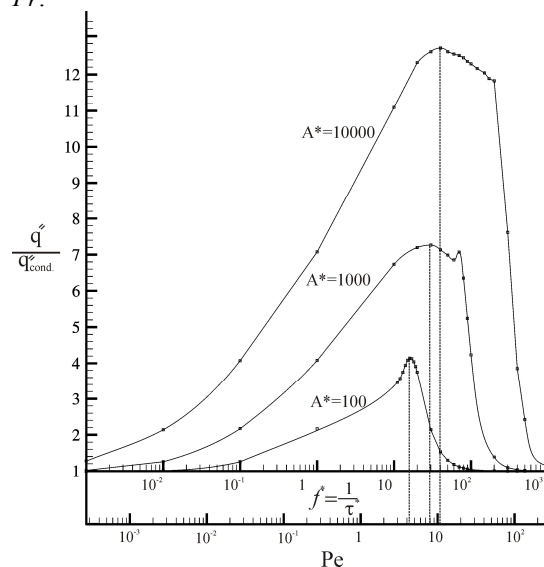


Fig 8: Effect of pressure gradient amplitude on non-dimensionalization heat flux.

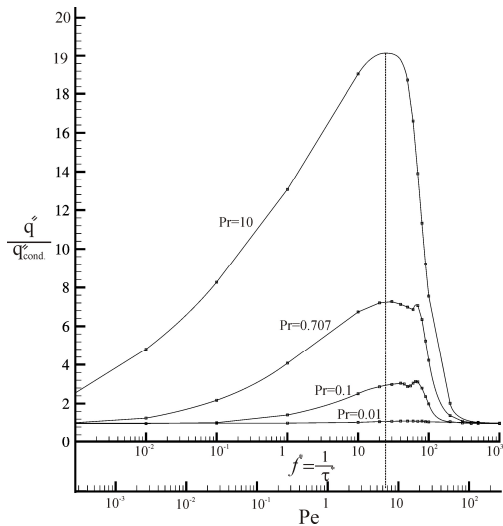


Fig 9: Effect of prandel number on non-dimensiolization heat flux.

Another matter is thermal developing. In flow with low Prandtel number, temperature distribution in the fluid is highly affected by temperature of other points in the field (because of dominance of diffusion term and ellipticity of governing equations) at this conditions much little time is needed to reach fully development. This fact can be seen from Fig.1 0.

VIII. Conclusion

Reciprocating forced convection flow has been studied. It is shown that for constant pressure gradient ($A^* = cte.$), non-dimensional parameters L_p and α will not be independent. It is found that at high values of α , Richardson annular effect become important and heat transfer will be enhanced. On the other hand high frequencies cause to sever decreasing the oscillations amplitude and penetration length. Reduction of penetration length, prevent the appropriate convection of the fluid under constant heat flux zone toward constant temperature boundaries and result reduction of heat transfer rate. In order to show this fact with an example, optimum frequency and geometry for maximization of heat transfer rate is investigated.

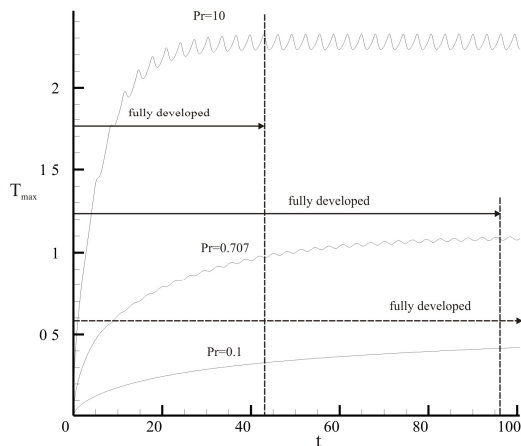


Fig 10: Effect of prandel number on thermal development.

At very high frequencies, oscillations amplitude is reduced and fluid has very small displacement. At very high frequencies the fluid becomes stationary conduction heat transfer will occurred. At very low frequencies, mechanism of heat transfer is nearly unidirectional forced convection. Since at this case Pe is a small number, when fluid changes direction, thermal developing is done quickly and so when $u \approx 0$ heat transfer mechanism is conduction. For a specified fluid, If higher value determined for A^* , maximum value is occurred at higher frequencies and in addition, because of Richardson annular effect, value of q/q_{max} is enhanced. On the contrary decreasing A^* , optimum point is shifted to lower frequencies and q/q_{max} is also decreased. Furthermore, geometrical parameters also might to be optimized, i.e., with constant L ($L_h + L_t = L = cte.$), optimum ratio of $r = L_H/L$ for maximum heat transfer rate has been obtained. By assumption of constant A and specific fluid, optimum values for L_p and α is obtained so the heat transfer rate be maximum. This procedure also can be done by numerical method of optimization such as genetic algorithm that in future works will be performed.

IX. References

- [1] Cooper, W. L., Nee, V. W., and Yang, K. T., 1994, "An Experimental Investigation of Convective Heat Transfer From the Heated Floor of a Rectangular Duct to a Low Frequency Large Tidal Displacement Oscillatory Flow," Int. J. Heat Mass Transf., 37, pp. 581–592.
- [2] Zhao, T., and Cheng, P., 1995, "A Numerical Solution of Laminar Forced Convection in a Pipe Subjected to a Reciprocating Flow," Int. J. Heat Mass Transf., 38, pp. 3011–3022.
- [3] Richardson, E. G., and Tyler, E., 1929 "The Transverse Velocity Gradient Near The Mouths of Pipes in Which An Alternating or Continuous Flow of Air is Established," Proc. Phys. Soc. London, 42, pp. 1–15.
- [4] Siegel, R., 1987, "Influence of Oscillation-Induced Diffusion on Heat Transfer in a Uniformly Heated Channel," ASME J. Heat Transfer, 109, pp 244–247.
- [5] Liao, Q. D., Yang, K. T., and Nee, V. W., 1995, "Microprocessor Chip Cooling by Channeled Zero- Mean Oscillatory Air Flow," Advances in Electronics Packaging, EEP-Vol. 10-2, pp. 789–794.
- [6] C. Sert, A. Beskok, "Numerical Simulation of Reciprocating Flow Forced Convection in Two-dimensional Channels", Journal of Heat Transfer, JUNE 2003, Vol. 125, pp. 403-412
- [7] G. E. Karniadakis and S.J. Sherwin. "Spectral/hp Element Methods for Computational Fluid Dynamic", 2nd ed. Oxford University Press, 2004.
- [8] A.T. Patera. A spectral element method for fluid dynamics: laminar flow in a channel expansion. *Journal of Computational Physics*, 54: 468–488, 1984.
- [9] C. Canuto, M.Y. Hussaini, A. Quarteroni, and T.A. Zang. "Spectral Methods in Fluid Dynamics", Springer-Verlag, New York, 1987.
- [10] P. Moin. "Fundamental of Engineering Numerical Analysis " Cambridge University Press, 2001.